

# Cost modelling and design optimisation of tidal stream turbines

Daniel S. Coles, Lucas. Mackie, David. White, and Jon. Miles

**Abstract**—A newly developed cost model for tidal stream turbines is presented. The model is based on (a) an existing tidal stream turbine cost model, (b) published CapEx data from an operational tidal stream turbine array, and (c) wind turbine cost data. The new cost model is utilised to establish cost-effective tidal stream turbine design, with the aim of reducing cost of energy through appropriate sizing of turbine rated power and rotor diameter for a given resource. A validated hydrodynamic model is used to estimate turbine energy yield at locations in Ramsey Sound, allowing cost of energy to be quantified. Drivers for cost reduction are identified and quantified. It is shown that optimal turbine placement and sizing can reduce turbine CapEx per unit energy by up to 40% on previously considered locations. The cost of ballast for gravity based foundations is also considered. Initial results show that through appropriate quantification of the effective friction between the gravity based structure and the seabed, the total gravity based structure cost can be reduced by up to 18%. Finally, we demonstrate how vessel costs can be reduced at relatively low flow sites such as Ramsey Sound as a result of longer duration slack tide periods.

**Index Terms**—Cost modelling, rated power, rotor diameter, turbine micro-siting, ballast, vessel cost, Ramsey Sound.

## I. INTRODUCTION

THE latest UK-wide tidal stream resource assessment, carried out by the Carbon Trust in 2011, reports a practical resource of between 21 - 34 TWh/year, with uncertainty bounds of -50%/+20% [1]. The practical resource is defined as the annual energy extraction that can be achieved once spatial, economic, environmental and grid constraints have been considered. Uncertainty in the practical resource estimate arise due to a lack of clarity over how the practical constraints should be defined. For example, the level of annual energy yield/turbine required to achieve economic viability is currently unclear, as it is reliant, and dependent on, the level of future subsidy support. More recent research concludes that the UK's tidal

D.S.C (email: daniel.coles@plymouth.ac.uk) and J.M acknowledge the financial support of the Tidal Stream Industry Energiser project (TIGER), co-financed by the European Regional Development Fund through the Interreg France (Channel) England Programme.

L.M acknowledges the financial support of an EPSRC PhD studentship award, grant number EP/R513052/1(18-22).

D.W acknowledges the financial support of the EPSRC (UK) Super-Gen Offshore Renewable Energy Hub (funding ref. EP/S000747/1).

D.S.C and J.M are with the School of Engineering, Computing and Mathematics, Faculty of Science and Engineering, University of Plymouth, Drake Circus, Plymouth, PL4 8AA, UK (e-mail: daniel.coles@plymouth.ac.uk)

L.M is with the Department of Earth Science and Engineering, Imperial College London, London, SW7 2AZ, UK

D.W is with the Faculty of Engineering and Physical Sciences, University of Southampton, Southampton, University Road, Southampton SO17 1BJ

stream energy resource could increase 7-fold if turbines can be installed at locations with spring tide velocities greater than 2 m/s, instead of 2.5 m/s [2]. The economic viability of sites with spring tide velocities of between 2 - 2.5 m/s must be considered to understand the potential increase in the practical resource that can practically be achieved.

This paper provides a new tidal stream turbine cost model. The cost model is based on an earlier model developed by Segura et al. [3], which is referred to in this paper as the Segura cost model. The accuracy of the Segura cost model is investigated using cost data published from the MeyGen project. Based on findings, the cost model is developed using published costs for common components used in wind turbines, such as gearboxes and generators. The new cost model is used to estimate the cost of existing tidal stream turbines that have been/are in operation, such as the Tidal Energy Ltd Deltastream, the Orbital Marine Power SR2000, and the SIMEC Atlantis AR1500. At this stage of investigation, the cost model considers the turbine only (i.e. all components in the nacelle, and the rotor blades and hub). A method for establishing cost-effective turbine design is presented. Ramsey Sound is used as a case study, where the performance of Tidal Energy Ltd's DeltaStream device is compared to alternative turbine designs. Finally, the new cost model is used to identify cost reduction drivers. First, the impact of turbine micro-siting on cost of energy is investigated. Second, the requirements for ballast are considered. Finally, the duration of slack tide periods are quantified in order to estimate vessel costs. Vessel cost comparisons are made between relatively low flow sites such as Ramsey Sound, and higher flow sites such as MeyGen.

The aim of this research is to build an understanding of the economic viability of tidal stream energy sites, to then update practical resource estimates. It also enables the key cost reduction drivers to be identified in order to inform the direction of future research and commercial activities.

## II. COST MODELLING

### A. Cost modelling

The Segura cost model [3] provides capital expenditure (CapEx) estimates for bed mounted, variable speed tidal stream turbines. The model defines cost functions for all main components in the turbine. Component costs are expressed as a function of component mass, turbine rated power, and/or rotor diameter. Components that contribute to the turbine cost include

the rotor blades, hub, pitch system, low speed shaft, high speed shaft, rotor core, main bearing, gear box, generator, main bearing, variable speed electronics, yaw system, mainframe, hydraulic system, cooling system, and the nacelle cover. Other costs that are included in the Segura cost model, but not considered here, include the cost of (a) project development, (b) the export cable, and (c) onshore infrastructure such as converters and transformers. Published cost data in these areas could not be sourced in order to assess the accuracy of the Segura cost functions. Turbine and gravity-base support structure cost functions from the Segura cost model are provided in Table I. The pitch system, low speed shaft and rotor core costs are all a function of the rotor radius. The rotor blades cost is a function of the rotor radius to the power of 2.7. The high speed shaft, main bearing, generator brake system, protection switch, cooling system and oil system costs are all a function of the turbine rated power. The gear box cost is a function of the turbine rated power to the power of 1.2. The cost of the yaw system, power take-off frame, control system, fairing, nacelle cover and all gravity based support structure components are independent of rotor radius and rated power, i.e. they are fixed costs that do not change with turbine sizing. It is unclear at this stage of investigation how valid these independent cost functions are.

To test the accuracy of the Segura cost model, the turbine cost of a MeyGen Phase 1A device, with rotor diameter of 18 m and rated power of 1.5 MW, was estimated, and compared with publicly available cost data [4]. It is reported that the cost of the four MeyGen Phase 1A turbines accounted for 39% (or £20 m) of the total CapEx of the project, which was £50 m. Assuming the turbine cost is split evenly between the four turbines, this is equivalent to £5 m/turbine. The Segura cost model estimates the turbine CapEx to be just £0.9 m, 85% lower than the reported CapEx. In the absence of component level CapEx data from MeyGen or any other project, it is not possible to establish if the Segura cost model is inaccurate in estimating all component costs, or if there are errors related to specific components. However, given the significant difference between the Segura model result and the MeyGen cost data, further development of the cost model is clearly required.

### B. New cost model

To improve the level of agreement with the MeyGen turbine CapEx data, a new cost model has been developed in this study. The new cost model is informed by cost data from wind turbines. Table II presents a summary of the main wind turbine component costs, as a proportion of the total turbine cost, based on estimates provided by the International Renewable Energy Agency (IRENA) [5]. The nine components account for 93% of the total turbine CapEx. The estimated component costs of a MeyGen Phase 1A turbine are also provided. These are simply calculated using the cost percentages of each component from wind relative to the total turbine CapEx, which in the case of MeyGen

Phase 1A turbines, we assume to be £5 m/turbine. The estimated MeyGen Phase 1A turbine component costs in Table II were used to derive correction factors to apply to the Segura cost functions in Table I. Table III summarises the new cost functions, with their correction factors, denoted by  $\phi$ . The cost functions for the power take-off frame and yaw system have been updated so that they are no longer fixed costs that are independent of turbine scale. Instead, these component costs are now linearly proportional to the turbine rated power. The Segura cost functions for all other components that do not feature in Table III remain unchanged.

Figure 1 shows the relationship between turbine rated power, rotor diameter, and estimated CapEx of (a) the rotor, (b) the power take-off system, (c) the auxiliary systems and (d) the whole turbine (i.e. the rotor, power take-off system and auxiliary systems) from the new cost model. Rotor components are a function of rotor diameter, whilst power take-off components are a function of turbine rated power. The auxiliary system components are a function of either rated power or rotor diameter.

Figure 2 shows the estimated cost of each component in a 1.5 MW, 18 m rotor diameter turbine, obtained from the new cost model. The cost of the blades make up the highest proportion of the total turbine cost, at approximately 40%. The next highest costs are from the gearbox and the generator, at around 22% and 6% respectively. The distribution of these costs will change depending on the scaling of turbine rated power and rotor diameter, so it is important to consider the distribution of these costs in the context of site specific constraints. This is done in Section III-B by considering the optimal design of a turbine located in Ramsey Sound, Wales.

The estimated cost of a MeyGen Phase 1A turbine, based on the new component cost functions, is £5.26 m, within 5% of the reported average MeyGen turbine cost. This level of agreement is unsurprising because cost functions for components that contribute significantly to the total turbine CapEx have been calibrated using the MeyGen cost data. This means there is high confidence that the new turbine cost model is accurate for a 1.5 MW, 18 m rotor diameter turbine, but validation is required over a range of turbine scales. It also does not provide evidence that individual component costs are being accurately estimated, only that the accumulated cost of all components show close agreement for one particular turbine design. Table IV provides the estimated turbine CapEx of devices that have been/are currently operating.

## III. COST OF ENERGY REDUCTION IN RAMSEY SOUND

### A. Resource characterisation

In this section the Ramsey Sound tidal stream energy resource is considered in order to investigate cost effective turbine design using the new cost model. Hydrodynamics in Ramsey Sound are characterised using a combination of Acoustic Doppler Current Profiler (ADCP) data, and outputs from a depth-averaged

TABLE I  
COMPONENT COST FUNCTIONS FROM THE SEGURA COST MODEL [3].

Component	Cost function	Description
<b>Turbine</b>		
Rotor blades	$N_b R_r^{2.7} C_b$	$N_b$ =number of blades, $R_r$ =rotor radius, $C_b$ =€40/m
Pitch system	$R_r C_{ps}$	$C_{ps}$ = €500/m
Low speed shaft	$R_r C_{lss}$	$C_{lss}$ = €500/m
High speed shaft	$P_t C_{hss}$	$C_{hss}$ = €300/MW
Rotor core	$R_r C_{cr}$	$C_{cr}$ = €1000/MW
Main bearing	$P_t C_{tb}$	$C_{tb}$ = €40,000/MW
Gear box	$P_t^{1.2} C_g$	$C_g$ = €35,000/MW
Generator	$P_t C_{eg}$	$C_{eg}$ = €180,000/MW
Brake system	$P_t C_{bs}$	$C_{bs}$ = €2,000/MW
Yaw system	$m_y C_{ys}$	$m_{ys}$ = 60 kg, $C_{ys}$ =€12/kg
Protection switch	$P_t C_{psw}$	$C_{psw}$ = €25,000/MW
Power take off frame	$m_{ptof} C_{ptof}$	$m_{ptof}$ = 3,600 kg, $C_{ptof}$ =€10/kg
Oil system	$P_t C_{pos}$	$C_{pos}$ = €15,000/MW
Cooling system	$P_t C_{cos}$	$C_{cos}$ = €15,000/MW
Condition monitoring system	$P_t C_{cms}$	$C_{cms}$ = €110,000/MW
Control system	$m_{cts} C_{cts}$	$m_{cts}$ = 30 kg, $C_{cts}$ =€12/kg
Electrical system	$P_t C_{psw} + m_{sc} C_{sc}$	$C_{psw}$ = €25,000/MW, $m_{sc}$ = 300 kg, $C_{sc}$ = €25/kg
Fairing	$m_f C_f$	$m_f$ = 1240 kg, $C_f$ =€10/kg
Nacelle cover	$m_{sd} C_{sd}$	$m_{sd}$ = 8 kg, $C_{sd}$ =€23,830/kg
<b>Gravity-base support structure</b>		
Base support	$m_{tbs} C_{tbs}$	$m_{tbs}$ = 87,200 kg, $C_{tbs}$ =€3/kg
Transition structure	$m_{tts} C_{tts}$	$m_{tts}$ = 39,500 kg, $C_{tts}$ =€3/kg
Vertical column	$m_{tvc} C_{tvc}$	$m_{tvc}$ = 29,800 kg, $C_{tvc}$ =€3/kg
Concrete ballast	$N_{cb} m_{cb} C_{cb}$	$N_{cb}$ = number of ballast blocks, $m_{cb}$ = 113,200 kg, $C_{cb}$ =€0.2/kg
Feet	$N_{bg} m_{bg} C_{bg}$	$N_{bg}$ = number of feet, $m_{bg}$ = 6,300 kg, $C_{bg}$ =€0.3/kg

TABLE II  
TYPICAL WIND TURBINE COMPONENT COSTS, AS A PROPORTION OF THE TOTAL TURBINE COST. ESTIMATES COSTS ARE FOR A MEYGEN PHASE 1A TURBINE.

Component	Cost proportion of total turbine cost	Estimated cost
Rotor blades	41.5%	£2.08 m
Gearbox	24%	£1.20 m
Generator	6.4%	£0.32m
Power take-off frame	5.2%	£0.26 m
Pitch system	5.0%	£0.25 m
Low speed shaft	3.6%	£0.18 m
Rotor hub	2.6%	£0.13 m
Main bearing	2.3%	0.12 m
Yaw system	2.3%	£0.12 m
<b>Total</b>	<b>92.9%</b>	<b>4.66 m</b>

coastal ocean model which has been previously developed and validated in [6]. The ADCP data was collected in 2009 at the location of the Tidal Energy Ltd DeltaStream turbine. The ADCP data is used to characterise the boundary layer profile at the turbine location. The ocean model employs coastal flow solver Thetis [7] (<http://thetisproject.org/>) and finite-element partial differential equation solver Firedrake [8] to solve the non-conservative form of the shallow-water equations. The domain, which encompasses a large section of the Irish sea, is discretised using an unstructured mesh domain generated with qmesh

[9] (<https://www.qmesh.org/>). Bathymetry is interpolated by combining 2 m measurements in the vicinity of Ramsey Sound [10] and coarser measurements elsewhere [11]. Ramsey Sound contains prominent and influential bathymetric features, namely a submerged pinnacle called Horse Rock, a rocky reef named “The Bitches” and a north-south trending trench. The location of these features, along with the bathymetry and distribution of time-averaged flow speeds are shown in Figure 3. A higher mesh refinement surrounding these features serves to accurately characterise both their geometry and impact on hydrodynamics. The model also makes use of bed class data [12] to apply a variable Manning coefficient field to compute bed shear stress. This field is scaled by 1.25 in Ramsey Sound to sufficiently calibrate the model against ADCP survey measurements.

The model provides insights into the flow characteristics of Ramsey Sound [6]. The asymmetry of the tide is apparent, with the flood tide producing tidal currents of higher velocity than the associated ebb tide currents. In addition, one can observe the influence aforementioned bathymetric features have in the shaping the flow fields. “The Bitches” causes a narrowing of the strait which increases flow velocities across a central channel. Meanwhile Horse Rock generates a prominent wake in this high velocity channel on the flood tide.

The model is used to establish the sensitivity of cost of energy to turbine location within Ramsey Sound. It is also used to quantify the duration of slack water

TABLE III  
NEW COMPONENT COST FUNCTIONS

Component	New cost function	Description
Rotor blades	$\phi_b N_b R_r^{2.7} C_b$	$\phi_b=53.5$ , $N_b$ =number of blades, $R_r$ =rotor radius, $C_b=\text{€}40/\text{m}$
Gearbox	$\phi_g P_t^{1.2} C_g$	$\phi_g=24$ , $C_g = \text{€}35,000/\text{MW}$
Generator	$\phi_{eg} P_t C_{eg}$	$\phi_{eg}=1.4$ , $C_{eg} = \text{€}180,000/\text{MW}$
Power take-off frame	$173000 P_t$	
Pitch system	$\phi_{ps} R_r C_{ps}$	$\phi_{ps}=66$ , $C_{ps} = \text{€}500/\text{m}$
Low speed shaft	$\phi_{lss} R_r C_{lss}$	$\phi_{lss}=46$ , $C_{lss} = \text{€}500/\text{m}$
Main bearing	$\phi_{tb} P_t C_{tb}$	$\phi_{tb}= 2.3$ , $C_{tb} = \text{€}40,000/\text{MW}$
Yaw system	$80000 P_t$	

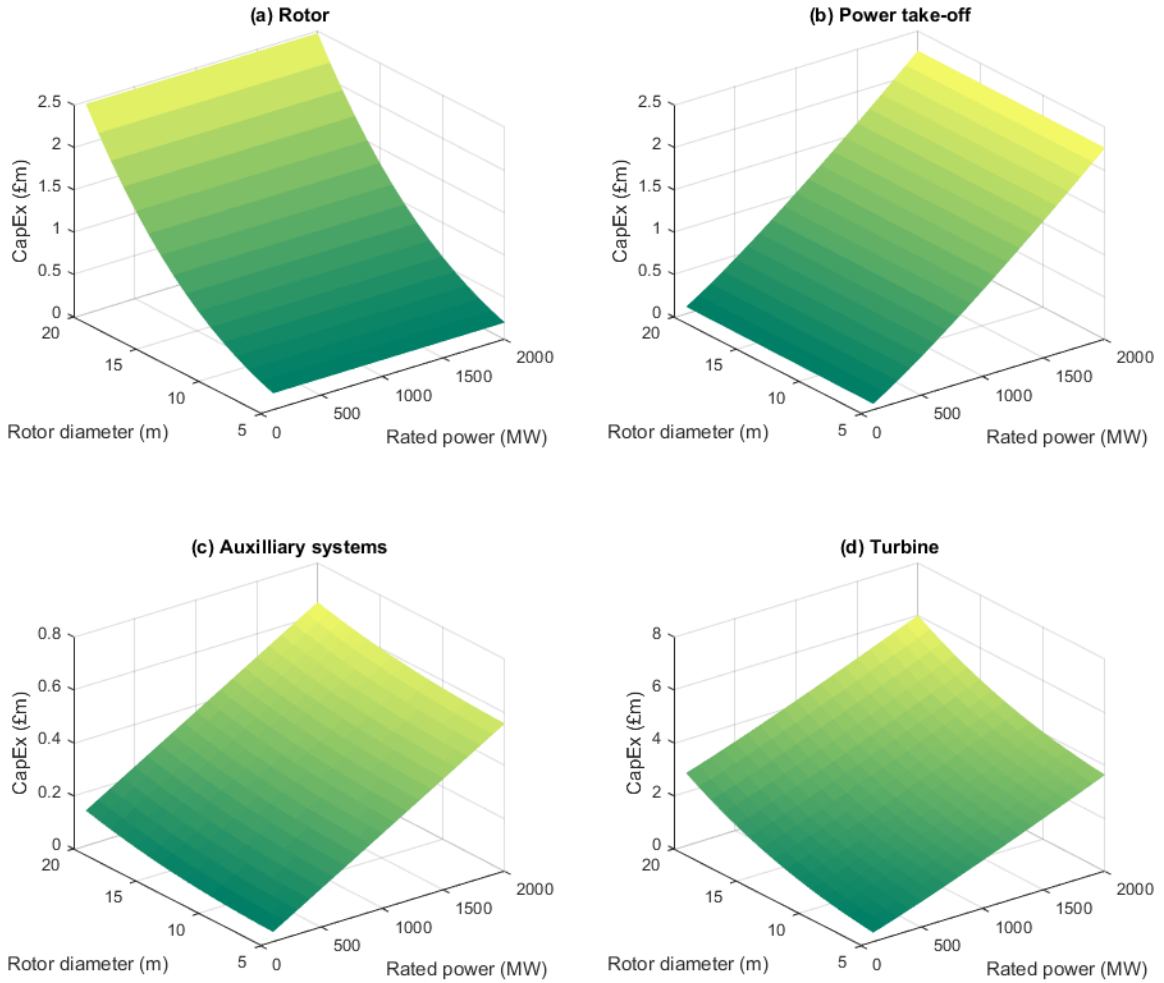


Fig. 1. Distribution of (a) turbine, (b) power take-off, (c) auxiliary systems and (d) total turbine cost, as a proportion of total turbine CapEx.

periods, in order to estimate vessel costs from offshore operations and maintenance.

### B. Turbine design and micro-siting

Figure 4 shows the relationship between rated power, rotor diameter and energy yield at the location of the Deltastream device, which is identified as 'DS' in Figure 3. When the objective is to minimise turbine CapEx per unit energy, the most economically

viable turbine design is a 0.4 MW device with 15 m rotor diameter. This achieves a turbine CapEx per unit energy of £82/MWh, based on the new cost model. This is demonstrated in Figure 5, which shows the relationship between rated power, rotor diameter and the ratio of turbine CapEx to 25 year energy yield. It is assumed that the turbine availability is 95%, and the project duration is 25 years. The turbines considered do not use a pitch system, to be consistent with the TEL

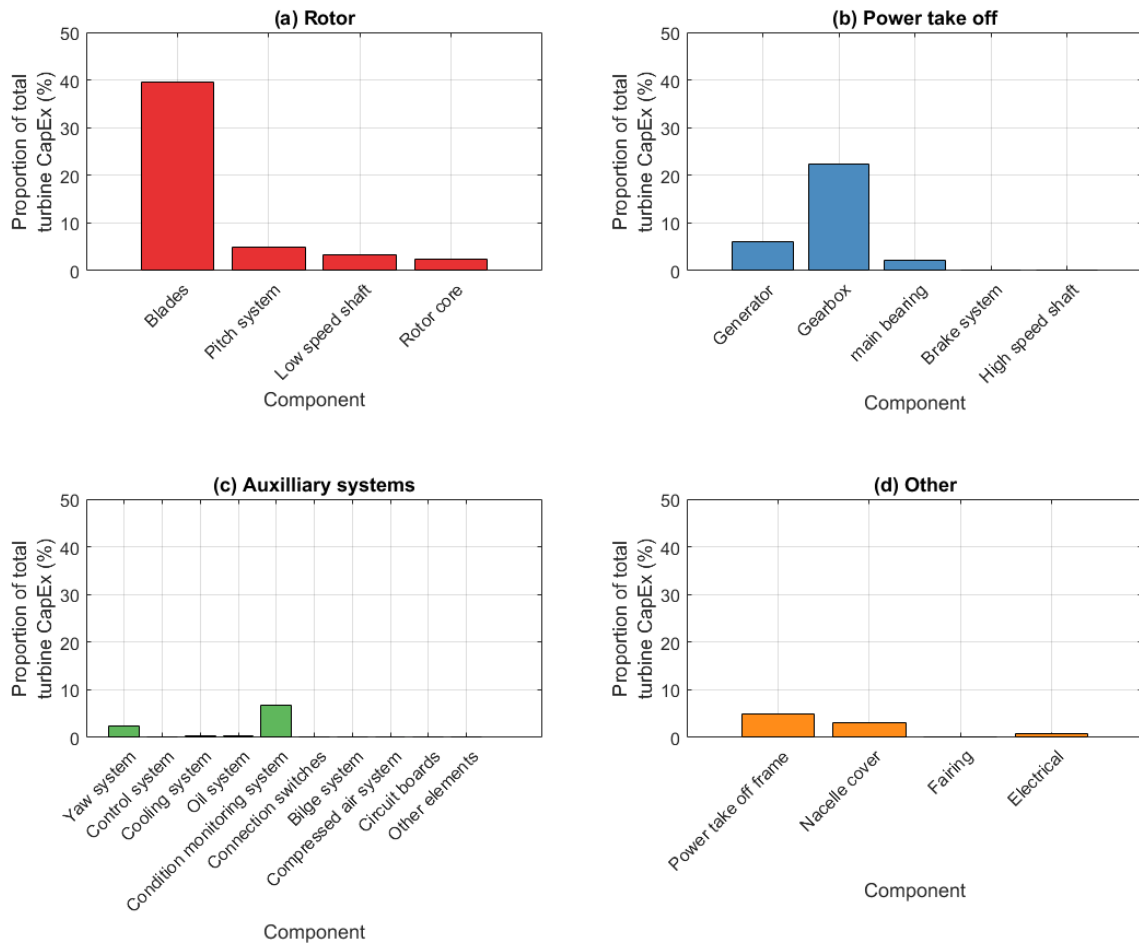


Fig. 2. Distribution of estimated (a) turbine, (b) power take-off, (c) auxiliary systems and (d) other costs of a 1.5 MW, 18 m rotor diameter turbine, as a proportion of total turbine CapEx

TABLE IV  
ESTIMATED TURBINE CAPEx FROM NEW COST MODEL.

Developer	Device	Rated power	Rotor diameter	Blades / rotor	Yaw system	Pitch system	Estimated turbine CapEx
Nova Innovation	M100-D	0.1 MW	8.5 m	2	No	Fixed	£0.49 m
Tidal Energy Ltd	Deltastream	0.4 MW	12 m	3	Yes	Fixed	£1.55 m
Alstom	DeepGen	1.0 MW	18 m	3	Yes	Variable	£4.34 m
Orbital Marine Power	SR2000	1.0 MW	16 m	2	No	Fixed	£2.90 m
Orbital Marine Power	O2	1.0 MW	20 m	2	No	Variable	£4.08 m
Andritz Hydro Hammerfest	HS1500	1.5 MW	18 m	3	Yes	Variable	£5.26 m
SIMEC Atlantis Energy	AR1500	1.5 MW	18 m	3	Yes	Variable	£5.26 m

Deltastream device. The 'optimal' device derived here is reasonably close to the design of the TEL DeltaStream device, which has a rated power of 0.4 MW, a rotor diameter of 12 m, and an estimated turbine CapEx per unit energy of £90/MWh. Differences between the 'optimal' turbine design derived here and the Deltastream device may arise because of additional costs incurred from the support structure, export cable, onshore infrastructure etc., which are not considered at this stage of investigation. Additionally, the high resolution flow data obtained from the Thetis model may provide an improvement on the flow data that was available at the time of the Deltastream design.

Selecting tidal turbine sites must consider both harnessing the kinetic energy from high velocity currents, whilst avoiding regions of high turbulence generated by bathymetric features and coastlines. Flow time series data was extracted from the Thetis model at three additional locations of interest for turbine deployment within Ramsey Sound. The locations, labelled DS, a, b and c are shown in Figure 3. The cumulative flow occurrence at the four locations is shown in Figure 6. Results show that highest flow speeds are exhibited at location c, where the depth at lowest astronomical tide (LAT) is 26.5 m. The DS location is deepest (31 m), with lowest flow speeds. Figure 7 shows a

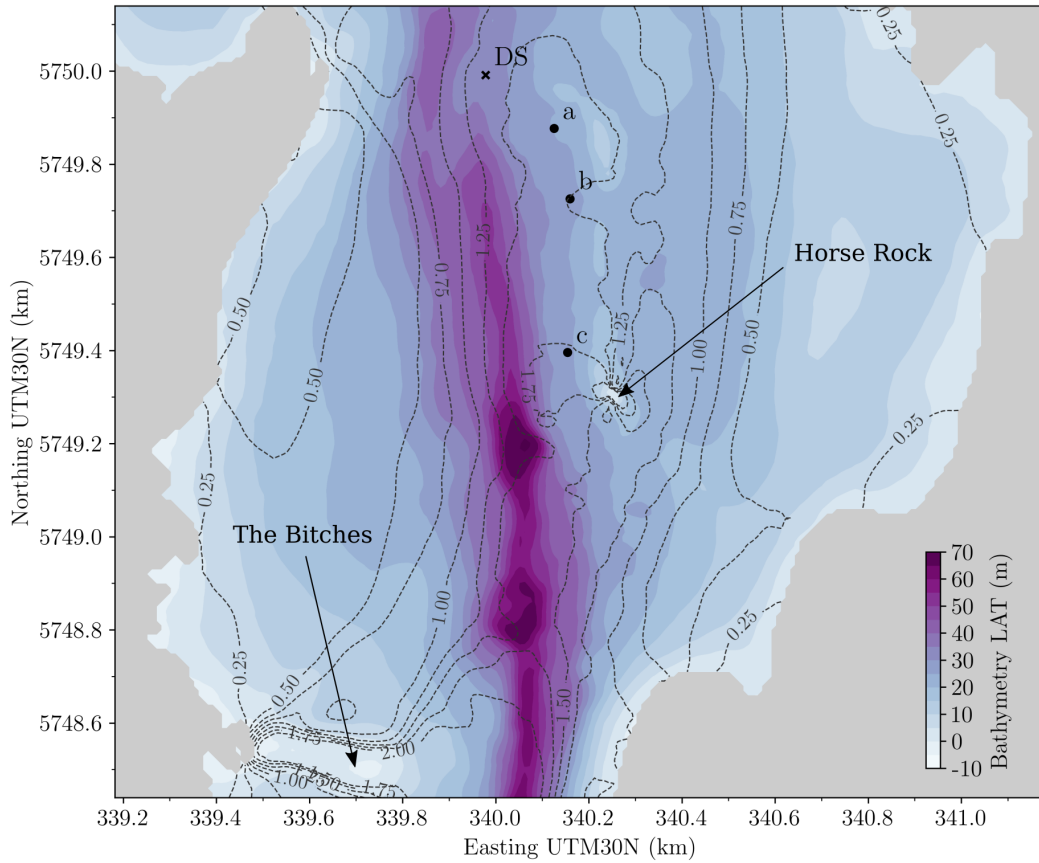


Fig. 3. Location of turbines within Ramsey Sound. Spatial variation in depth (LAT) and time-averaged flow speeds (dotted contours) are also shown.

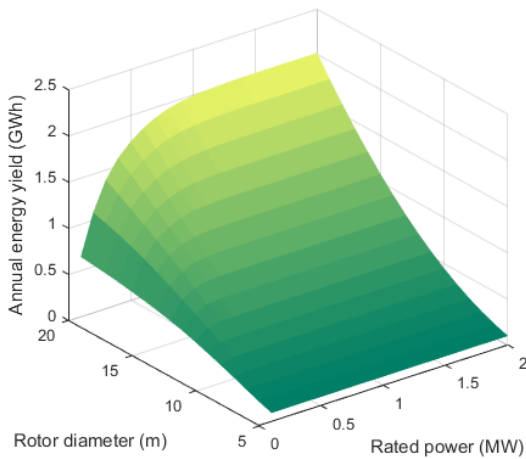


Fig. 4. Relationship between rated power, rotor diameter, and annual energy yield.

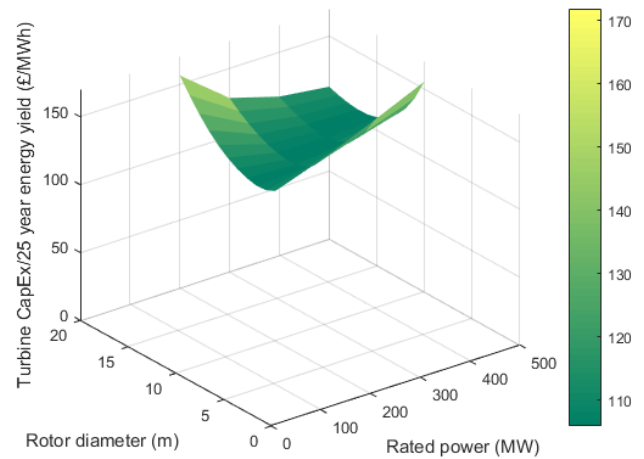


Fig. 5. Relationship between Rated power, rotor diameter and the ratio of turbine CapEx and 25 year energy yield at the global minimum.

depth averaged flow speed time series at the four locations during a spring tide. Locations a, b and c show greater asymmetry between flood and ebb flow speeds than at DS, with higher flow speeds occurring during flood tides. Location c exhibits the greatest level of asymmetry between flood and ebb flows. This may be as a result of the proximity to Horse Rock. Locations a and b are located west of a shallow region that is also likely to influence flow speeds during flood tides. Asymmetry in flow speeds between flood and ebb is

not uncommon at tidal stream energy sites, however the differences seen here may impact detrimentally on fatigue loading that would require components such as the blades and the GBS to be structurally reinforced, at additional cost. It may be that the revenue from any uplift in energy yield outweighs the increased CapEx required for structural reinforcements. Whilst this is out of the scope of this paper, work is ongoing to investigate the suitability of the flow in Ramsey Sound

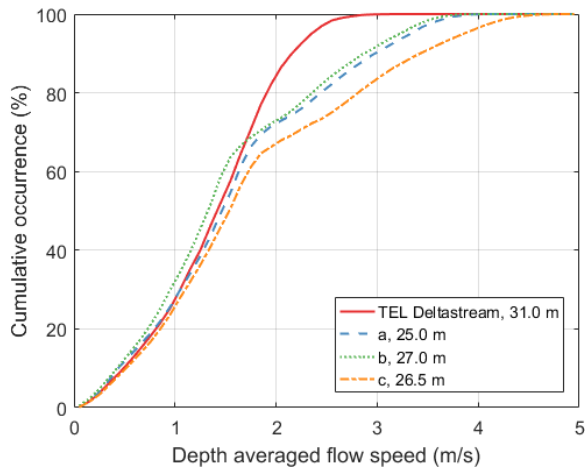


Fig. 6. Relationship between depth averaged flow speed and occurrence at four locations in Ramsey Sound

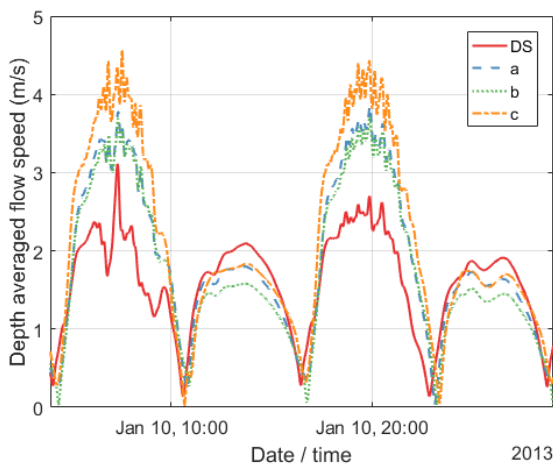


Fig. 7. Depth averaged flow speed timeseries at locations DS, a, b and c in Ramsey Sound.

TABLE V  
ESTIMATED ANNUAL POWER PERFORMANCE OF THE TEL DELTASTREAM AT DIFFERENT LOCATIONS IN RAMSEY SOUND.

Turbine location	Annual energy yield	Capacity factor
DS	0.81 GWh	0.23
a	1.18 GWh	0.34
b	1.08 GWh	0.31
c	1.36 GWh	0.39

for turbine deployment.

The annual energy yield of TEL DeltaStream devices (i.e. rated power of 0.4 MW and rotor diameter of 12 m) at each location was estimated, with results presented in Table V. Results highlight the significant spatial variation in the energy resource within Ramsey Sound. It is estimated that a Deltastream device at location c can achieve a capacity factor of 0.39, 70% higher than at the DS location.

To establish the most cost-effective turbine design at locations a, b, and c, the method implemented for the DS location was repeated. A constraint on rotor diameter was implemented to ensure a minimum clearance

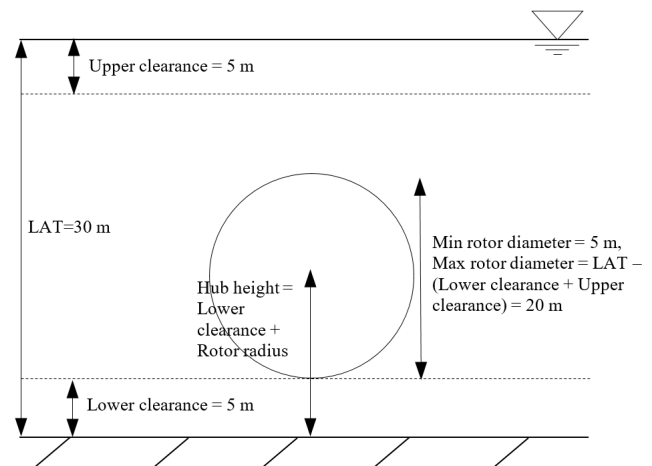


Fig. 8. Rotor diameter constraint.

between the rotor and the seabed, as well as the rotor and the free surface at lowest astronomical tide, of at least 5 m. This is illustrated in Figure 8.

Table VI provides results from the analysis. The most cost effective solution, in terms of turbine CapEx per unit energy, is achieved at location c, using a 0.7 MW turbine with a 12 m rotor diameter. This achieves a turbine CapEx per unit energy of £49/MWh. Importantly, this is a 40% reduction on the turbine CapEx/energy yield of the optimal turbine at the DS location. The turbine CapEx per unit energy at locations b and c lie between those achieved at DS and c. Both turbines have a power rating of 0.6 MW and a rotor diameter of 13 m.

Results presented here demonstrate the potential for cost of energy to be reduced significantly through optimal turbine design and micro-siting. To achieve this, accurate hydrodynamic modelling of sites is required to characterise the spatial variation in the ambient flow.

As arrays increase in size, it is likely that a single turbine design will be used in order to utilise economies of volume from manufacturing. In this case the same process of turbine design optimisation must be carried out, with consideration for array blockage which slows the flow in the vicinity of the array [13]. This is out of the scope of this paper, but is an area of further work being planned.

### C. Ballast

A further opportunity for cost reduction, relating to gravity-based structures (GBS), is raised in the following section. Most shallow tidal stream sites have hard rocky seabeds, so the support structure is either founded on a heavy gravity base, designed to resist sliding and overturning failure, or on large diameter piles that are drilled into the seabed. As an example, gravity-based support structures were adopted by the MeyGen project. Each turbine is on a support structure that weighs 250-350 tonnes with an additional 1,200 tonnes of ballast in the form of two 200 tonne steel ballast blocks on each of the three legs. The total dry mass of 1500 tonnes corresponds to a submerged weight of 13 MN. MeyGen reported that the substructure CapEx

TABLE VI  
ESTIMATED ANNUAL POWER PERFORMANCE OF THE TEL DELTASTREAM AT DIFFERENT LOCATIONS IN RAMSEY SOUND.

Turbine location	Rated power	Rotor diameter	Turbine CapEx	Annual energy yield	Turbine CapEx/25 yr energy yield
DS	0.4 MW	15 m	£2.4 m	1.2 GWh	£82/MWh
a	0.6 MW	13 m	£2.3 m	1.6 GWh	£58/MWh
b	0.6 MW	13 m	£2.3 m	1.5 GWh	£64/MWh
c	0.7 MW	12 m	£2.2 m	1.9 GWh	£49/MWh

accounted for 11% of the total CapEx of the project [4]. Drilled piles require a more costly installation process than a GBS, but have been adopted in some cases, such as the Seagen project in Strangford Lough. In this case, a 2x2 group of piles was drilled into the seabed to support the steel sub-structure.

On rocky seabeds, the sliding capacity,  $H_{ult}$ , of a GBS is expressed simply using a sliding friction limit of:

$$H_{ult}/V = \tan(\delta) \quad (1)$$

where  $V$  is the vertical force transmitted through the foundation base and  $\delta$  is the foundation-seabed interface friction angle. This simple approach is not sufficient on sandy or clayey soils because in partially-drained or undrained conditions the vertical force may be partly carried by pore water pressure. This reduces the effective stress carried by the soil skeleton, and therefore the available inter-particle friction. The potential for pore pressure build-up is considered in GBS design for sandy and clayey seabeds, and is evident in large scale GBS tests, such as the campaign for an offshore wind GBS foundation reported by [14]. However, on rock, pore pressure effects can generally be ignored.

Design codes do not offer detailed advice on the interface friction angle appropriate for a GBS-rock interface. For general soil conditions – focused on sand or clay – the previous version of the DNV geotechnical design code recommended  $\tan\delta$  be limited to 0.4. The most recent update of this code has removed this limit and recommends instead that a suitable value be derived from laboratory measurements.

The interface friction angle,  $\delta$ , can be measured in the laboratory using rock samples and representative concrete or steel interface plates. In this type of test the two materials are prepared as planar surfaces. For example, [15], [16] present results for different rock and interface materials, showing results in the range  $0.1 < \tan\delta < 0.9$ .

There is an additional effect that should be considered when scaling from a laboratory test on planar interfaces to a GBS resting on the seabed: the ruggedness of the seabed, and potentially also the GBS underside. Recent studies related to cable stability on rocky seabeds have shown that the effective friction coefficient, defined by the horizontal and vertical forces acting at the point of contact, is also influenced by the local seabed slope at this point [17]. Since real rocky seabeds have rugged features of varying scales, there is generally a variation in this slope among the

different contact points where a cable is supported by the seabed. The overall effect is an increase in the average lateral resistance on the cable, and therefore an improvement in the hydrodynamic stability [18]. The model used to assess cable-seabed friction on sloping rock is as set out by [19], who considered the friction of rock joints that have a sawtooth profile.

If the local slope of the rock at the point of contact is  $\theta$  then the effective friction is:

$$H_{ult}/V = \tan(\delta + \theta) \quad (2)$$

This same effect is worth considering for GBS structures. A GBS is much larger than a cable, and also larger than the ruggedness features generally found on a rock seabed. As a result, the contact points between the underside of a rigid flat precast GBS and a rocky seabed will generally be horizontal, so  $\theta = 0^\circ$ , and the capacity  $H_{ult}$ , given by equations 1 and 2 is equal. However, if the base of the GBS includes grouting, which conforms to the seabed ruggedness, or if the GBS underside has other irregular or conformable elements, then some level of sawtooth effect will exist, and the effective foundation friction will be increased. All of these GBS-seabed interface types, smooth, irregular or serrated and concrete grouted, have been used in previous GBS trials for offshore wind [20]. There exists wide experience of rock joint interface strength from the wider literature, for example related to the stability of excavations in rock or concrete dams founded on rock. Models for rock joint strength have extended the sawtooth effect to also allow for failure of the rock (or concrete) material itself, through models such as Barton's approach [21]. This model introduced the joint roughness coefficient (JRC) to describe the undulations of the interface. The JRC is analogous to the ruggedness of the seabed and the GBS underside, in this context.

By combining the sawtooth and JRC models, the enhancement of GBS sliding resistance due to seabed ruggedness can be estimated. Such estimates depend on the assumed GBS-seabed interface type and the realism of scaling from rock joint undulations to seabed ruggedness, which generally involves larger features. The relevant GBS-seabed contact depends on the profiles of the seabed and the GBS underside, and any grouting used. Here, an illustrative example is based on a GBS-rock interface friction angle of  $\delta = 30^\circ$ , i.e.  $\tan\delta=0.58$  and a contact point slope of  $10^\circ$ . This value is slightly greater than the shallower faces of sawtooth profiles reported for shoreline rock outcrops [15], and would be a low estimate for a contact points on

displacement of a rigid grouted base on such rugged seabeds. For typical rock properties, the Barton JRC strength is not exceeded, and instead it is the Patton sawtooth criterion that governs, raising the effective friction from 0.58 to 0.84.

To illustrate the design efficiency from this increase in effective friction, the Segura cost model and TEC system has been used. The TEC system considered by Segura *et al.* (2017) is a 1.2 MW device with 20 m rotor diameter. It is supported on a steel tripod GBS with concrete ballast blocks and underbase concrete grouted bags. The base case design is assumed to give a certain sliding capacity,  $H_{ult}$ , based on a conventional friction of 0.58. If an enhanced friction of 0.84 is assumed, the same lateral sliding capacity can be achieved without needing the 226 tonnes (dry weight) of concrete ballast blocks and the tripod weight can be reduced by 16 tonnes. Based on the Segura cost model, these adjustments reduce the cost of the support structure by 18%. There would also be a reduction in the cost of TEC installation, because of the reduced number of lifting operations, as well as the potential reduction in the required lifting capacity and therefore a reduction in vessel specification.

This example is purely illustrative, and further data and research is required to validate any enhancement of the design sliding capacity from seabed ruggedness. The adoption of higher rock joint friction through similar physical mechanisms in other areas of civil engineering, as well as recent work on power cable stability, suggests this is a promising approach.

#### D. Vessel cost

For projects using bed mounted tidal stream turbines, operations and maintenance costs are driven predominately by the requirement for dynamic positioning vessels. Dynamic positioning vessels perform offshore operations accurately and safely over a range of weather conditions. The vessels are leased at a cost of between c. £30,000 - £80,000/day. The vessel day rate is driven by the demand for vessels, which can depend on vessel demand from the oil and gas, and offshore wind sectors.

Operations carried out on tidal stream energy projects that require large/advanced vessels include cable laying, and the deployment/retrieval of support structures, ballast, and turbines. These operations typically require the use of remotely operated vehicles (ROV) that use on-board cameras to provide a visual aid for the operations. ROVs typically operate in flows below 1 m/s, as flow higher than this cause excessive drag, preventing the ROV from being able to hold station. This limits the duration operations can take place to slack windows, when flows fall below 1 m/s. For this reason neap tides are usually targeted for offshore operations to be undertaken, when slack windows are at their longest. Slack window duration is also dependent on site specific flow behaviour, where high flow sites exhibit shorter slack windows than low flow sites.

Figure 9 compares the percentage of time that depth averaged flow speeds occur at point locations in Ram-

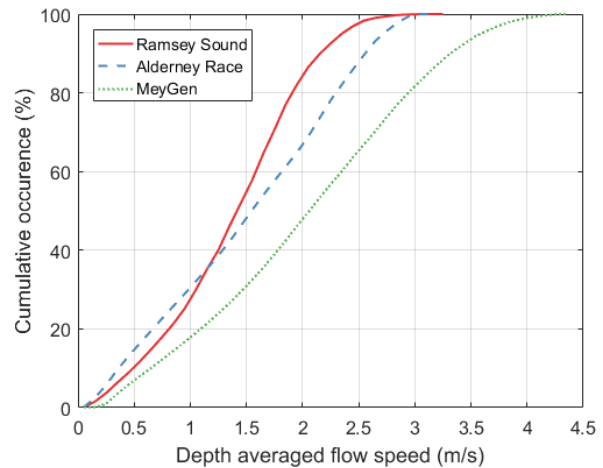


Fig. 9. Relationship between depth averaged flow speed and occurrence, using time series data from Ramsey Sound, Alderney Race and MeyGen.

sey Sound, the Alderney Race, and MeyGen. Depth averaged flow speeds were extracted from validated hydrodynamic models over a spring-neap period. Results presented here are representative of a single location at each site, so do not account for the spatial variability in flow speeds at each site. It is acknowledged that the flow speeds in regions of the Alderney Race reach similar levels recorded at MeyGen, and so these initial results are provided for demonstrative purposes. The depth averaged flow speed at Ramsey Sound and Alderney Race falls below 1 m/s approximately 30% of the time. At MeyGen, this reduces to approximately 18% of the time. The average duration of slack tide periods, defined here as the period that the depth averaged flow speed is less than 1 m/s, at Ramsey Sound, the Alderney Race and MeyGen, is 102 minutes, 113 minutes and 66 minutes respectively. At Ramsey Sound and Alderney Race, over 100 x 1 hour operations could potentially take place per month, whilst at MeyGen this reduces to 60/month, a reduction of 40%. At Ramsey Sound and the Alderney Race, approximately 50% of the slack water periods exceed a duration of 1 hour. At MeyGen, this drops to 26%.

Table VII provides a summary of findings from the slack tide analysis. Figure 10 provides a comparison of the operational window durations at Ramsey Sound, Alderney Race and MeyGen. The spring tide occurs half way through the time period plotted, when the shortest operational windows occur. At Ramsey Sound, the duration of the operational windows drops below 1 hour after 16 operational windows. In this period, there are seven operational windows that are less than 1 hour at MeyGen.

The duration of slack tide periods is a key driver of vessel cost, where longer duration slacks provide the opportunity for more work to be carried out per slack, and for successive slacks to be utilised for operations. This increases the likelihood of being able to complete offshore operations during the neap tide periods when slack tides are at their longest. Failure to achieve this may mean having to return the vessel and completing

the operations during the following neap tide period, or waiting for the next available operating window. This will incur significant additional cost as a result of the additional vessel time required. For example, if it is assumed that 20 separate operations need to be undertaken, and each operation requires a minimum of 1 hour, the estimated number of days required at Ramsey Sound, Alderney Race and MeyGen, based on the data presented in Figure 9, is 7 days, 5 days and 13 days respectively. This assumes that the vessel cannot be returned during spring tide and then leased again. Assuming a vessel day rate of £40,000/day, the total vessel cost is £280,000, £200,000 and £520,000. Depending on the vessel day rate, these costs can vary significantly, but demonstrate the sensitivity of vessel cost on flow speed.

#### IV. CONCLUSIONS

A new tidal stream turbine cost model has been developed, based on an existing model (the Segura cost model [3]), cost data from wind turbines, and published turbine CapEx data from the MeyGen project [4]. The new cost model overestimates the average CapEx of a MeyGen Phase 1A turbine by 5%. Validation of the cost model over the range of turbine scales considered in this paper is ongoing. The new cost model has been used to demonstrate a method for establishing cost effective turbine design through selection of the most suitable rated power and rotor diameter. Based on the tidal stream energy resource in Ramsey Sound, the turbine CapEx per unit energy of the TEL DeltaStream device is estimated to be £90/MWh. This improves to £82/MWh by increasing the rotor diameter to 15 m. Further improvements to turbine performance are achieved through optimal micro-siting and turbine design, where a 0.7 MW, 12 m rotor device located to the south-east of the Deltastream achieves a turbine CapEx per unit energy of £49/MWh. Additional cost of energy drivers have been investigated. These include the necessity for ballast once appropriate friction between the GBs and the seabed is considered. Initial results indicate that the CapEx of the support structure may reduce by around 18%, assuming an increase in sliding friction of 45% is representative for grouted GBS feet with sawtooth interaction with the sea bed. Finally, it is shown that at relatively low flow sites such as areas of Ramsey Sound and the Alderney Race, long duration slack windows may allow vessel hire costs to be reduced significantly relative to higher energy sites, due to the higher frequency of long duration slack windows with flows below 1 m/s for a minimum duration of 1 hour.

#### V. FURTHER WORK

Work is ongoing to validate the new tidal stream turbine cost model against real data over a range of turbine scales. The model will be applied to a range of sites around the UK to test their economic viability based upon site-specific resource characteristics. The new cost model will also be extended to include the gravity based foundation costs. An investigation into

micro-siting of turbines within Ramsey Sound is also ongoing, with additional consideration for flood-ebb asymmetry and its implications on turbine design and cost.

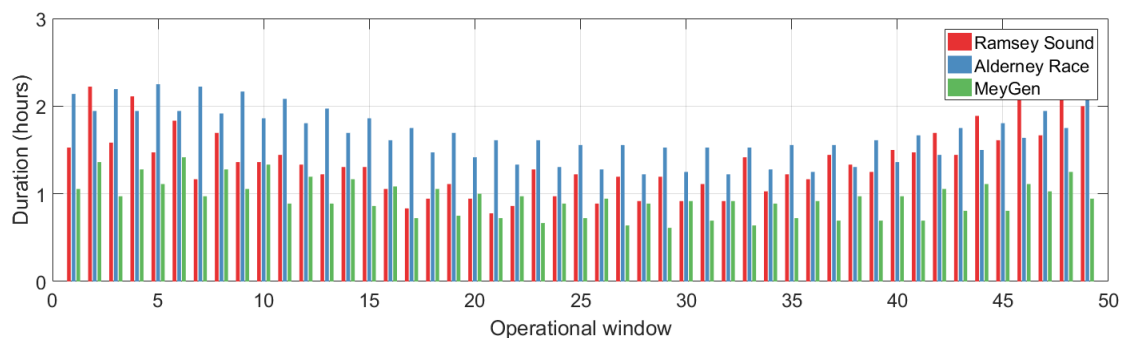


Fig. 10. Slack water durations at points in Ramsey Sound, the Alderney Race and MeyGen.

TABLE VII  
SLACK WATER CHARACTERISTICS AT LOCATIONS IN RAMSEY SOUND, THE ALDERNEY RACE AND MEYGEN.

Site	% time < 1 m/s	Average slack tide period	Number of slack tides > 1 hour
Ramsey Sound	27.4%	102 minutes	102 (44%)
Alderney Race	30.5%	113 minutes	115 (50%)
MeyGen	17.9%	66 minutes	60 (26%)

## REFERENCES

- [1] The Carbon Trust, "UK Tidal Current Resource & Economics," Tech. Rep. July, 2011. [Online]. Available: [https://www.carbontrust.com/media/77264/ctc799{\\\_}uk{\\\_}tidal{\\\_}current{\\\_}resource{\\\_}and{\\\_}economics.pdf](https://www.carbontrust.com/media/77264/ctc799{\_}uk{\_}tidal{\_}current{\_}resource{\_}and{\_}economics.pdf)
- [2] M. Lewis, S. Neill, P. Robins, and M. Hashemi, "Resource assessment for future generations of tidal-stream energy arrays," *Energy*, vol. 83, pp. 403–415, 2015.
- [3] E. Segura, R. Morales, and J. A. Somolinos, "Cost assessment methodology and economic viability of tidal energy projects," *Energies*, vol. 10, no. 11, pp. 1–27, 2017.
- [4] Black and Veatch, "Lessons Learnt from MeyGen Phase 1A Final Summary Report," Tech. Rep., 2020.
- [5] International Renewable Energy Agency, "Renewable Energy Technologies: Cost analysis series. Volume 1: Power sector. Wind power," Tech. Rep. 5/5, 2012.
- [6] L. Mackie, P. S. Evans, M. J. Harrold, T. O'Doherty, M. D. Piggott, and A. Angeloudis, "Modelling an energetic tidal strait: investigating implications of common numerical configuration choices," *Applied Ocean Research*, vol. 108, no. January, p. 102494, 2021. [Online]. Available: <https://doi.org/10.1016/j.apor.2020.102494>
- [7] T. Kärnä, S. C. Kramer, L. Mitchell, D. A. Ham, M. D. Piggott, and A. M. Baptista, "Thetis coastal ocean model: discontinuous Galerkin discretization for the three-dimensional hydrostatic equations," *Geoscientific Model Development*, vol. 11, no. 11, pp. 4359–4382, 2018.
- [8] F. Rathgeber, D. A. Ham, L. Mitchell, M. Lange, F. Luporini, A. T. McRae, G. T. Bercea, G. R. Markall, and P. H. Kelly, "Firedrake: Automating the finite element method by composing abstractions," *ACM Transactions on Mathematical Software*, vol. 43, no. 3, 2016.
- [9] A. Avdis, A. S. Candy, J. Hill, S. C. Kramer, and M. D. Piggott, "Efficient unstructured mesh generation for marine renewable energy applications," *Renewable Energy*, vol. 116, pp. 842–856, 2018. [Online]. Available: <https://doi.org/10.1016/j.renene.2017.09.058>
- [10] Bangor University, "UKHO Tide Gauge Data Network," Tech. Rep., 2017.
- [11] Seazone Solutions Ltd, "Edina Digimpa Service. Hydrospatial one. Gridded bathymetry," Tech. Rep., 2014.
- [12] British Geological Survey, "BGS Geology: marine sediments 250k — DigSBS250," Tech. Rep., 2011.
- [13] D. S. Coles, L. S. Blunden, and A. S. Bahaj, "The energy yield potential of a large tidal stream turbine array in the Alderney Race: Energy yield estimate for Alderney Race," *Philosophical Transactions of the Royal Society A: Mathematical, Physical and Engineering Sciences*, vol. 378, no. 2178, 2020.
- [14] G. Sedlacek, A. Mieke, A. Libreros, and Y. Heider, "Geotechnical stability of gravity base foundations for offshore wind turbines on granular soils," in *Proceedings of the International Conference on Offshore Mechanics and Arctic Engineering*, vol. 4, Rio de Janeiro, Brazil, 2012, pp. 57–63.
- [15] A. Ziogos, M. Brown, A. Ivanovic, and N. Morgan, "Interface shear characteristics of Scottish rock samples from sites with tidal energy potential," in *Proceedings of the XVI ECSMGE Geotechnical Engineering for Infrastructure and Development*, Edinburgh, Scotland, 2015, pp. 793–798.
- [16] —, "Chalk – steel interface testing for marine energy foundations," *Proceedings of the Institution of Civil Engineers - Geotechnical Engineering*, vol. 170, no. 3, pp. 285–298, 2016.
- [17] T. Griffiths, W. D.J., S. Draper, L. Cheng, A. Leighton, and A. Fogliani, "Lateral resistance of 'rigid' pipelines and cables on rocky seabeds," *Canadian Geotechnical Journal*, vol. 56, no. 6, pp. 823–839, 2019.
- [18] T. Griffiths, D. White, S. Draper, F. Johnson, D. Coles, S. Ingham, C. Lourie, L. Cheng, and A. Fogliani, "Subsea cable stability on rocky seabeds – back analysis of field observations against recent research predictions," in *Proc. Conf. on Ocean, Offshore & Arctic Engineering*, Madrid, Spain, 2018, pp. Paper OMAE2018–77130.
- [19] F. Patton, "Multiple modes of shear failure in rock," in *Proc. 1st Congr. Int. Soc. Rock Mech*, Lisbon, Portugal, 1966, pp. 509–513.
- [20] M. D. Esteban, J. S. López-Gutiérrez, and V. Negro, "Gravity-based foundations in the offshore wind sector," *Journal of Marine Science and Engineering*, vol. 7, no. 3, 2019.
- [21] N. Barton, "Review of a new shear-strength criterion for rock joints," *Engineering Geology*, vol. 7, no. 4, pp. 287–332, 1973.